PAPER

Borane-tethered heteroscorpionate zinc catalysts for the hydroboration of carbon dioxide, isocyanates, esters and nitriles†

Tiago F. C. Cruz ✦* and Luís F. Veiros ✦

This work describes the synthesis, characterization and catalytic hydroboration activity of a family of zinc bis(κ^2-borohydride) complexes containing borane-functionalized heteroscorpionate ligands. The new zinc bis(κ^2-borohydride) complexes with R-substituted bis(3,5-dimethylpyrazolyl)methane ligands with or without borane functionalities **[(L1−4)Zn(BH$_4$)$_2$] 1−4** (**1**, R = H; **2**, R = CH$_2$CH=CH$_2$; **3**, R = CH$_2$CH$_2$CH$_2$(9-borabicyclo[3.3.1]nonane) or CH$_2$CH$_2$CH$_2$(9-BBN); **4**, R = CH$_2$CH$_2$CH$_2$BCy$_2$) were synthesized by reacting the corresponding dichloride complexes **[(L1−4)ZnCl$_2$]** with two equivalents of NaBH$_4$ in THF. The new complexes were characterized by NMR spectroscopy, FTIR spectroscopy and elemental analysis, while complex **3** was characterized by single-crystal X-ray diffraction. The borane-functionalized complexes **3** and **4** catalyzed the hydroboration of CO$_2$ at 1 bar pressure, an array of isocyanates and esters and the dihydroboration of a set of nitriles with pinacolborane (HBPin) at catalyst loadings of 1 mol% and temperature of 60 °C in yields of 32−99%. In the cases of CO$_2$ and isocyanates, the methylated products (along with PinBOBPin) were preferred after 16 h. The catalytic reactions utilizing 1 mol% of the unfunctionalized complexes **1** and **2** achieved yields in the range of 7−24%, an average 4-fold decrease in catalytic activities, confirming that the catalytic intermediates benefit from the intra- or intermolecular stabilization of incorporated boranes.

Introduction

The selective reduction of inexpensive unsaturated molecules containing heteroatoms such as oxygen or nitrogen is of great importance in organic chemistry, as it paves the way to the synthesis of alcohols or amines, respectively, being often of added value to the fine chemistry sector. Substrates such as carbon dioxide (CO$_2$), isocyanates, esters and nitriles, which are also readily available, fall into such a category.

Among the ways to achieve chemical reduction, hydroboration is one of the most sought after, because not only does it avoid the harsh reaction conditions of hydrogenation and hydrosilylation processes, but also formally incorporates a borane moiety on the respective unsaturation products, thus creating molecules containing new heteroatom–boron bonds. Such synthons are very important classes of reagents because they pave the way to carbon–heteroatom bond formation *via* stereospecific tandem cross-coupling or oxidation processes

(Chart 1A).[1] CO$_2$ hydroboration using pinacolborane (HBPin) as the borane source has been catalyzed by several systems based on transition metals such as Mn,[2] Fe,[3] Co,[4] Ni,[5] Cu,[6] Mo,[7] Ru,[8] and Pd[9] or main group elements.[10] Among these, only particular cases have selectively produced the methyl boronate ester product H$_3$COBPin[11] resulting from the triple reduction of CO$_2$. The hydroboration of isocyanates has been catalyzed by transition metals such as Co,[12] Cu,[13] and Ag,[14] main group elements[15] and rare earth[16] elements, in which, depending on the catalytic conditions used, formamide or methylamide levels of chemical reduction can be achieved. Regarding the hydroboration of esters with HBPin, relevant works have been very few, with most catalysts reported being those based on molecular compounds of the main group elements, such as aluminum and lithium.[17] Lastly, the dihydroboration of nitriles with HBPin has been widely covered in the literature, being catalyzed by complexes containing transition metals such as Mn,[18] Fe,[19] Co,[20] Ni,[21] Ru,[22] and Ag[23] or main group[24] and rare-earth elements.[25] Among all the systems discussed above, only selected complexes have served as multitasking catalysts, in which multiple families of substrates were readily converted: KHBEt$_3$ has been known to hydroborate isocyanates as well as esters,[26] while some other systems catalyzed the hydroboration of both nitriles and esters (Chart 1B).[27]

Centro de Química Estrutural, Institute of Molecular Sciences, Departamento de Engenharia Química, Instituto Superior Técnico, Universidade de Lisboa, Av. Rovisco Pais, 1049 001 Lisboa, Portugal. E-mail: carpinteirocruz@tecnico.ulisboa.pt
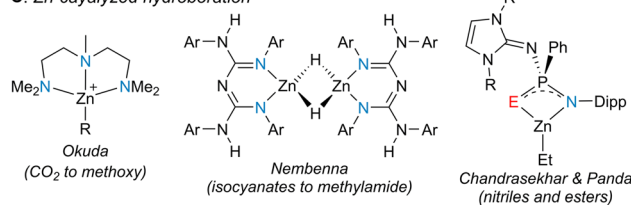†Electronic supplementary information (ESI) available. CCDC 2401462. For ESI and crystallographic data in CIF or other electronic format see DOI: https://doi.org/10.1039/d4dt03363a

A: *Hydroboration of CO₂, isocyanates, esters and nitriles*
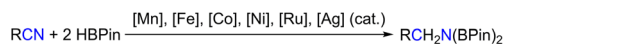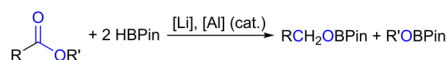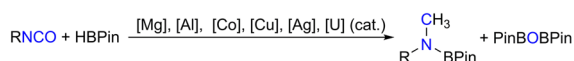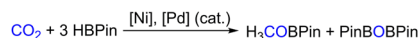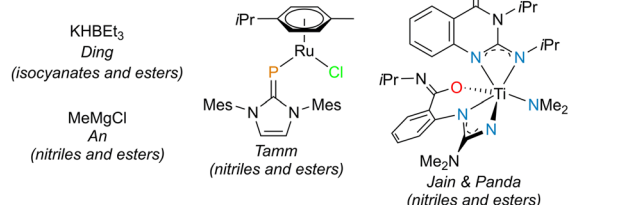
Chart 1 Catalyst systems reported for the hydroboration of CO₂ (methoxy level of reduction), isocyanates (methylamide level of reduction), esters and nitriles with HBPin (A), catalyst systems used in the reduction of multiple families of substrates with HBPin (B), selected cases of zinc-catalyzed hydroboration with HBPin (C), and examples of borane-functionalized coordination spheres (D). Abbreviations Mes, Dipp and 9-BBN denote mesityl (2,4,6-trimethylphenyl), 2,6-diisopropylphenyl and 9-borabicyclo[3.3.1]nonane, respectively.

Zinc-catalyzed CO_2 hydroboration with HBPin has featured formate and methoxy selectivities.[28] The hydroboration of isocyanates catalyzed by zinc complexes has been reported by Nembenna and coauthors with a conjugated bis(guanidinate) zinc hydride complex, in which the catalytic products resulting from mono, double and triple reduction of the isocyanates were selectively obtained by using 1, 2 or 3 equivalents of HBPin as the borane source, respectively.[29] Zinc-catalyzed dihydroboration of nitriles has also been featured in the literature,[30] while Panda and coworkers have reported tri-coordinated zinc alkyl complexes with N^E (E = S and Se) frameworks capable of catalyzing the dihydroboration of nitriles and the hydroboration of esters (Chart 1C).[31]

The manipulation of secondary coordination spheres in transition metal complexes has led to important influences on their catalytic ability and, therefore, is of paramount importance in the field of homogeneous catalysis.[32] Manipulating secondary coordination spheres with boranes has the advantage of achieving *push–pull* reactivity,[33] in which the borane acts as a Lewis acid and a ligand within the coordination sphere of a transition metal complex acts as a Lewis base, thus being further activated (Chart 1D). Bercaw or Klankermayer and respective coworkers used borane–phosphine ligands to activate hydride/carbonyl ligands in some transition metal complexes.[34] Drover and coworkers extended this approach by reporting borane-functionalized 1,2-bis(phosphino)ethanes, which have been featured in the preparation of numerous transition metal complexes,[35] one such system catalyzing the hydroboration of benzonitrile with HBPin.[36] Szymczak and coworkers functionalized pyridinepyrazolyl,[37] 1,4,7-triazacyclononane[38] or cyclic (alkyl)(amino)carbene[39] derivatives with boranes and studied the chemistry of their respective transition metal coordination complexes, with applications in stoichiometric and catalytic small-molecule activation. Werlé and coworkers functionalized a phosphino triazine chelate with borane and its respective transition metal complexes were used as catalysts in the hydrogenation of nitroarenes or the synthesis of silyl enol ethers.[40]

In previous work, we reported new bis(3,5-dimethylpyrazolyl)methane ligands functionalized with pendant boranes and the chemistry of their respective coordination processes with zinc.[41] In that work, we realized that the dichloride complexes **[(L1–4)ZnCl₂]** (see Scheme 1), upon activation with 2 equivalents of KHBEt₃, were active catalysts for the hydroboration of CO_2 with HBPin, with complete selectivity to H₃COBPin in a maximum yield of 86%. In that work, the complexes that exhibited the best results were those adorned with borane functionalities (that is, complexes **[(L3,4)ZnCl₂]**). In those cases, the intramolecular stabilization of the hydride/formate catalytic intermediates by the pendant borane functionalities was behind their amplified catalytic activities.

Picking up from our previous findings, and to avoid the pre-activation of the dichloride complexes with KHBEt₃, we detail in the present report the synthesis and characterization of a new family of zinc bis(κ^2-borohydride) complexes **[(L1–4)Zn(BH₄)₂] 1–4** (see Scheme 1), and their activity as multitasking catalysts in the hydroboration of CO_2, isocyanates, esters and nitriles.

Results and discussion

The bis(κ^2-borohydride) zinc complexes **[(L1–4)Zn(BH₄)₂] 1–4** bearing bis(3,5-dimethylpyrazolyl)methane (**L1**, R = H) or its allyl (**L2**, R = CH₂CH=CH₂) or borane (**L3**, R = CH₂CH₂CH₂(9-borabicyclo[3.3.1]nonane) or CH₂CH₂CH₂(9-BBN) and **L4**, R = CH₂CH₂CH₂BCy₂) functionalized derivatives were prepared by the reaction of the previously isolated dichloride complexes **[(L1–4)ZnCl₂]** [41,42] with two equivalents of NaBH₄ in THF (Scheme 1).
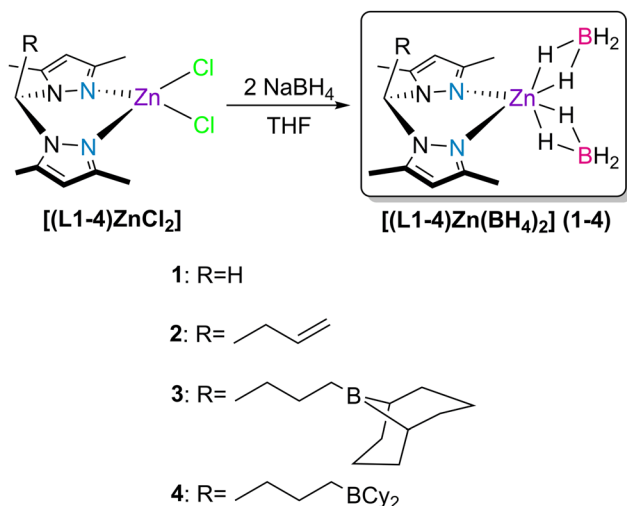
**Scheme 1** Synthesis of the bis(κ^2-borohydride) zinc complexes **1–4**.

Complexes **3** and **4** were also isolated in good yields *via* post-*anti*-Markovnikov hydroboration of the allylated complex **2** with the 9-BBN dimer or dicyclohexylborane, respectively, in dichloromethane for 2 h and at 25 °C. The post-hydroboration reactions of **2** with diphenylborane, dimesitylborane or bis(pentafluorophenyl)borane (Piers' borane) resulted in untraceable mixtures. Complexes **1–4** are insoluble in *n*-hexane and diethyl ether and soluble in toluene, THF and dichloromethane and were characterized by NMR and FTIR spectroscopies and elemental analysis. The spectra of all complexes are presented in Fig. S1–S16 in the ESI.† The NMR spectra of the complexes display the expected resonances for the moieties present in compounds **L1–4**. The CH resonance of the 3,5-dimethylpyrazolyl rings in the ligands are downfield-shifted upon coordination to zinc, going from 5.76–5.77 ppm to 6.08–6.15 ppm. Similarly, the methyl resonances in the 3,5-dimethylpyrazolyl moieties go from being seemingly overlapped at 2.19 ppm in ligands **L1–4** to two distinct, upfield-shifted resonances at 2.41–2.52 ppm upon coordination to zinc. This latter fact is in line with the decrease in the symmetry of ligands **L1–4** caused by the coordination strain of the respective bis(3,5-dimethylpyrazolyl)methyl moieties. The complexes exhibit respective proton borohydride resonances centered at 0.42–0.49 ppm as broad quartets, arising from coupling of the ^{1}H and ^{11}B nuclei ($^1J_{BH}$ = 83–84 Hz). Additionally, the ^{11}B resonances in these complexes are quintets at −42.9 to −45.7 ppm, with $^1J_{BH}$ = 83–85 Hz. These observations are indicative of the existence of borohydride moieties in the complexes.[43] Complexes **3** and **4** also present ^{11}B NMR resonances in the range of 82.9–87.4 ppm, characteristic of tricoordinate boranes simultaneously containing alkyl and 9-BBN/BCy$_2$ fragments.[44]

The FTIR spectra of complexes **1–4** revealed the presence of two strong broad bands at 2450–2200 cm^{-1} and 2200–2000 cm^{-1}, respectively, attributed to terminal and bridging B–H stretching in the borohydride ligands. In addition, strong bands in the range of 1100–1110 cm^{-1} were also

observed in all complexes, corresponding to BH$_2$ deformation. These results are in line with the spectral observations made for complexes containing κ^2-BH$_4$ ligands.[45] Furthermore, the presence of 9-BBN or BCy$_2$ and propylenic moieties in complexes **3** and **4** was characterized by an increase of the intensity of C–H bond vibration modes in the 2750–3000 cm^{-1} range with respect to the unfunctionalized complexes **1** and **2**.

Complex **3** was analyzed by single-crystal X-ray diffraction, having crystallized in the monoclinic system, in the $P2_1$ space group. Owing to the poor quality of the single crystal obtained for complex **3**, its molecular structure is only presented as a proof of connectivity in Fig. 1 while its selected bond lengths and angles and crystallographic data are displayed in Tables S1 and S2 in the ESI.†

Complex **3** demonstrates a κ^2-*N,N* coordination mode of ligand **L3**, as well as two κ^2-BH$_4$ co-ligands. The borane arm is also evident in its molecular structure, where the three-carbon hydrocarbyl bridge between the bis(pyrazolyl)methane and the 9-BBN moieties adopt a staggered conformation. The two fused 6-membered rings of the 9-BBN moiety in complex **3** adopt a boat–boat configuration. The Zn1–N bond lengths are in the range of 2.017(18)–2.052(15) Å and the Zn1–B distances in complex **3** are in the range of 2.250(19)–2.260(20) Å. The coordination geometry of complex **3** is a distorted pseudo-tetrahedron; the τ_4 parameter[46] is equal to 0.92 when considering the N1, N3, B2 and B3 atoms as the edges of the tetrahedron centered on the Zn1 atom. The chelation ring in complex **3** adopts a boat configuration, where the α and β ring puckering parameters,[47] defined as the angles between the {N1, N2, N3, N4} and {C11, N2, N4} and {N1, N2, N3, N4} and {Zn1, N1, N3} planes, are equal to 53.56° and 7.89°, respectively. Complex **3** is, to the best of our knowledge, the first crystallographically reported zinc bis(κ^2-borohydride) complex with a bis(pyrazolyl) ligand motif. Three other zinc bis(κ^2-borohydride) complexes have been reported in the literature, and their Zn–B distances are in the range of 2.252–2.355 Å,[48] which are within those found for complex **3**. The X-ray struc-
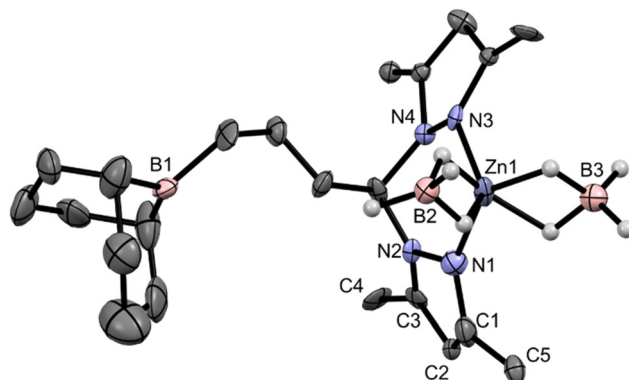
Fig. 1 Proof of the molecular connectivity of complex **3** determined by single-crystal X-ray diffraction, showing 30% probability ellipsoids. All hydrogen atoms, except those of the borohydride ligands, have been omitted for clarity.

ture of complex **3** was accurately reproduced by DFT calculations, as highlighted by the respective structure superimpositions presented in Fig. S17 in the ESI.†

With fully characterized complexes **1–4** in hand, they were tested in the hydroboration of different families of substrates. The first substrate to be tested in a hydroboration reaction with HBPin catalyzed by complexes **1–4** was CO_2, given our previous results using complexes [(**L1–4**)ZnCl₂] as precatalysts,[41] the results of which are summarized in Table 1.

As indicated in Table 1, performing the hydroboration of CO_2 in C_6D_6 at 1 bar and 60 °C catalyzed by 1 mol% of complexes **1–4** led to HBPin conversion rates of 18–34%, increasing in the following order: **1** < **2** < **3** ≈ **4** (Table 1, entries 1–4). The hydroboration of CO_2 catalyzed by the currently reported complexes selectively gave rise to the formation of the methyl boronate ester $H_3COBPin$, along with PinBOBPin, with their formation detected by ^{1}H NMR spectroscopy, matching the data found in the literature.[49] This result indicates that the borane functionalities present in complexes **3** and **4** are beneficial for their catalytic activity. Furthermore, when performing the hydroboration of CO_2 in THF-d_8 using complex **3** as a catalyst, the HBPin conversion increased to 57%, somewhat improving the previously obtained result using the catalyst system composed of [(**L3**)ZnCl₂]/2KHBEt₃ (Table 1, entries 5 and 6).

Given the success of the single-component system catalysts **1–4** in converting CO_2 with HBPin, other isoelectronic heteroallenes were sought after, such as *N,N′*-dicyclohexylcarbodiimide and *tert*-butyl isocyanate. When using 1 mol% of complexes **1–4** at 60 °C, *tert*-butyl isocyanate was hydroborated with HBPin, as summarized in Table 2.

Table 2 shows that complexes **1–4** achieved HBPin conversions of 9–35% after 1 h of reaction, increasing in the order **1** < **2** < **4** < **3** (Table 2, entries 1–4). This again indicates that the borane functionalities present in complexes **3** and **4** are beneficial for their catalytic activity. The catalytic reactions performed in the presence of complexes **3** and **4** were accompanied by the observation of hydroboration products resulting from different degrees of *tert*-butyl isocyanate

Table 1 Hydroboration of CO_2 with HBPin catalyzed by complexes **1–4**[a]

$$CO_2 + 3\ HBPin \xrightarrow[\text{60 °C, 16 h, solvent}]{\text{1 mol\% of cat.}} H_3COBPin + PinBOBPin$$

Entry	Cat.	Solvent	Conversion[b] (%)
1	**1**	C_6D_6	18
2	**2**	C_6D_6	24
3	**3**	C_6D_6	34
4	**4**	C_6D_6	32
5	**3**	THF-d_8	57
6	[(**L3**)ZnCl₂][c]	THF-d_8	42[d]

[a] Conditions: 1 mol% cat.; 1 mmol of HBPin; 1 bar of CO_2. [b] Conversions were determined by ^{1}H NMR spectroscopy utilizing 1,3,5-trimethoxybenzene as an internal standard and based on HBPin. [c] 2 equivalents of KHBEt₃ added. [d] Ref. 41.

Table 2 Hydroboration of *tert*-butyl isocyanate with HBPin catalyzed by complexes **1–4**[a]

$$tBuNCO + 3\ HBPin \xrightarrow[\text{60 °C, time, } C_6D_6]{\text{1 mol\% of cat.}}$$

(+ PinBOBPin)
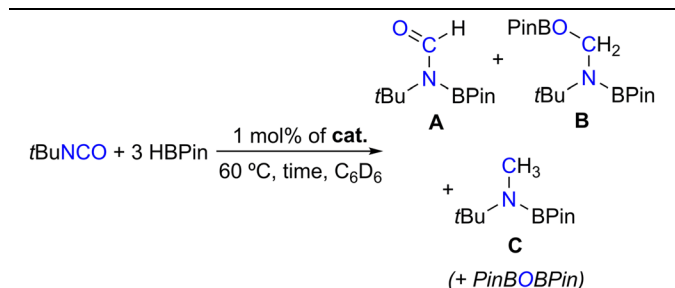
Entry	Cat.	Time (h)	Conversion[b] (%)	A : B : C ratio[b]
1	**1**	1	9	1 : 0 : 0
2	**2**	1	10	1 : 0 : 0
3	**3**	1	35	1.8 : 0 : 1
4	**4**	1	26	7.1 : 0 : 1
5	**3**	16	>99	0 : 0 : 1

[a] Conditions: 1 mol% cat.; 0.5 mmol of HBPin; 0.5 mmol of *tert*-butyl isocyanate. [b] Conversions and product ratios were determined by ^{1}H NMR spectroscopy by relative integration of the resonances of the HBPin and products and were based on HBPin.

reduction: formamide (**A**), methanamide (**B**) and methylamide (**C**) levels, the latter also concomitantly forming with PinBOBPin, in **A** : **B** : **C** ratios equal to 1.8–7.1 : 0 : 1. The formation of the hydroboration products of *tert*-butyl isocyanate was detected by ^{1}H NMR spectroscopy, matching the data found in the literature,[12] and their ratio was calculated by relative integration of the respective resonances. When performing the hydroboration of *tert*-butyl isocyanate with HBPin using 1 mol% of complex **3** for 16 h at 60 °C, the reaction proceeded to full conversion with exclusive selectivity toward the methylated product **C**, along with PinBOBPin (Table 2, entry 5). Performing the same reactions using 1 or 2 equivalents of HBPin with respect to *tert*-butyl isocyanate did not change the selectivity in the products of catalysis. Under the same reaction conditions, *N,N′*-dicyclohexylcarbodiimide remained unreactive.

To further understand the reactivity profile of the hydroboration of *tert*-butyl isocyanate with HBPin catalyzed by 1 mol% of complex **3**, the reaction conversion and yields were monitored over time at 60 °C (Fig. 2).

The reaction conversion and yield monitoring of the hydroboration of *tert*-butyl isocyanate with HBPin at 60 °C catalyzed by 1 mol% of complex **3** over time led to the detection of compounds **A**, **B** and **C** (and PinBOBPin) at early reaction times (<30 minutes), with compound **B** being only observed in trace amounts. Compound **A** reached a maximum yield of 8% after 2 h and gradually disappeared, thus converting to compound **C**. After 6 h of the reaction, compound **C** (along with PinBOBPin) is the only observable product and achieved the maximum yield after 7.5 h. The maximum TOF of this reaction, measured at the highest rate of HBPin conversion, is equal to 33 h⁻¹. The conversion profile of the hydroboration of *tert*-butyl isocyanate catalyzed by complex **3** is somewhat analo-

Fig. 2 Conversion and yield monitoring of the hydroboration of *tert*-butyl isocyanate with HBPin catalyzed by **3** over time at 60 °C: evolution of the conversion of HBPin (blue data) and the yields of the boramidate products resulting from the mono (red data), double (yellow data) and triple (green data) reduction of *tert*-butyl isocyanate, that is, products **A**, **B** and **C** in Table 3, respectively. The colored lines are a visual guide. Conditions: 1 mol% of **3**; 0.5 mmol HBPin; 0.5 mmol *tert*-butyl isocyanate; solvent: C_6D_6 (0.5 mL). The conversions and yields were determined by ^{1}H NMR spectroscopy by relative integration of the resonances of the HBPin and boramidate products.

gous to that observed for the hydroboration of CO_2 catalyzed by complex [(L3)ZnCl$_2$]/2KHBEt$_3$, meaning that the methylamide product was sequentially formed from the formamide and methanamide ones. The system [(L3)ZnCl$_2$]/2KHBEt$_3$ also catalyzed the hydroboration of *tert*-butyl isocyanate, selectively forming the corresponding methyl boramidate product in quantitative yield. This latter result is though misleading, considering that KHBEt$_3$ itself is an efficient isocyanate hydroboration catalyst[26] and using complex [(L3)ZnCl$_2$] on its own did not achieve any recordable conversion after 16 h at 60 °C.

The new complexes **1–4** also catalyzed the hydroboration of ethyl benzoate, giving rise to the respective benzyl and ethyl boronic esters, as indicated in Table 3.

By looking at Table 3, the hydroboration of ethyl benzoate catalyzed by 1 mol% of complexes **1–4** for 16 h at 60 °C led to conversions of 7–52%, increasing in the following order, **1** < **2** < **4** < **3** (Table 3, entries 1–4), again indicating the relevance of the borane functionality to the catalytic activity. In addition, when using complex **3** as a catalyst, the HBPin conversion decreased to 15% when performing the reaction for 1 h (Table 3, entry 5).

The last substrate to be preliminarily screened for hydroboration using complexes **1–4** as catalysts was diphenylacetonitrile and the respective catalytic results are presented in Table 4.

Table 4 indicates that only complexes **3** and **4** functioned as good catalysts for the dihydroboration of diphenylacetonitrile, leading to the formation of the corresponding boramidate, achieving 75% conversion after 1 h at 60 °C (Table 4, entries 3 and 4), while complexes **1** and **2** did not lead to conversions higher than 15% (Table 4, entries 1 and 2). This follows the trend already observed for the substrates considered above. Full conversion of diphenylacetonitrile was achieved using complex **3** as a catalyst by extending the reaction time to 16 h (Table 4, entry 5). The formation of the imine PinBN=CH (CHPh$_2$), resulting from the monohydroboration of diphenylacetylene with HBPin was never observed throughout all hydroboration runs, even when employing stoichiometric amounts of HBPin.

As disclosed so far, 1 mol% of complex **3** was able to catalyze the hydroboration of CO_2, *tert*-butyl isocyanate, ethyl benzoate and diphenylacetonitrile. Taking this into account, the substrate scope of this catalyst system was explored under the optimized conditions. In effect, 1 mol% of complex **3** successfully catalyzed the hydroboration of a variety of isocyanates and esters and the dihydroboration of nitriles, as summarized in Scheme 2.

Complex **3** selectively catalyzed the hydroboration of a set of isocyanates. Several aliphatic and electronically differentiated aromatic isocyanates, including 1-isocyanatonaphthalene, were successfully reduced to the respective methyl bora-

Table 3 Hydroboration of ethyl benzoate with HBPin catalyzed by complexes **1–4**[a]

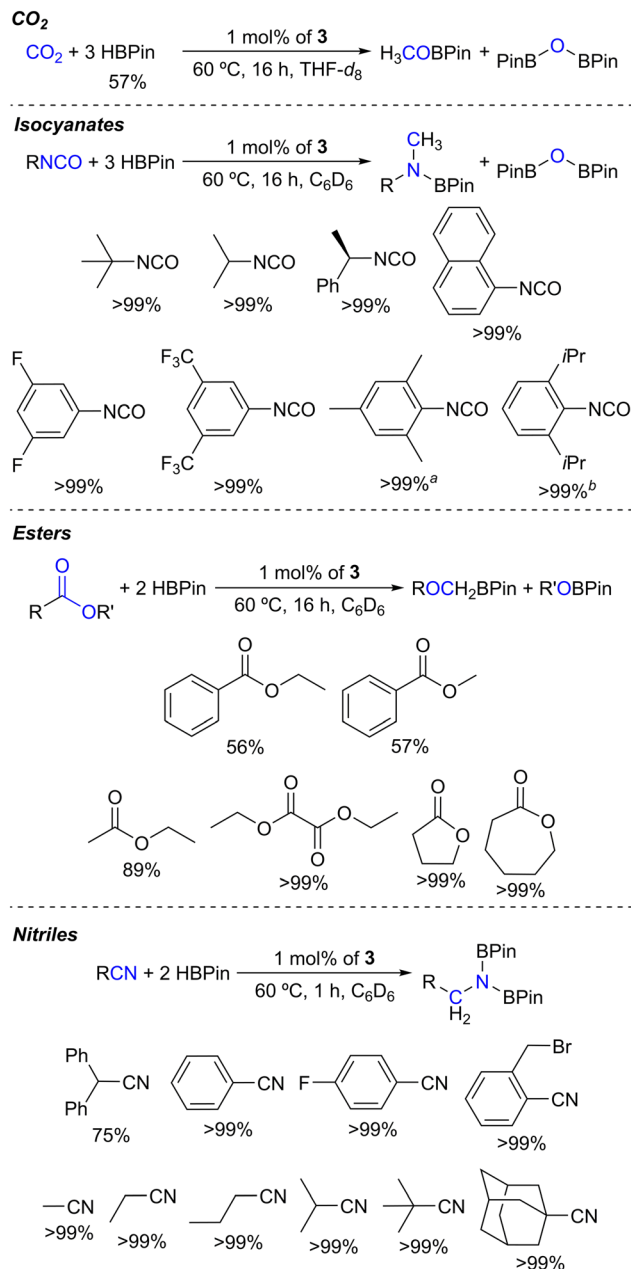| Entry	Cat.	Time (h)	Conversion[b] (%)
1	**1**	16	7
2	**2**	16	11
3	**3**	16	52
4	**4**	16	29
5	**3**	1	15

[a] Conditions: 1 mol% cat.; 0.5 mmol of HBPin; 0.5 mmol of ethyl benzoate. [b] Conversions were determined by ^{1}H NMR spectroscopy by relative integration of the resonances of the HBPin and products and were based on HBPin.

Table 4 Dihydroboration of diphenylacetonitrile with HBPin catalyzed by complexes **1–4**[a]

Entry	Cat.	Time (h)	Conversion[b] (%)
1	**1**	1	7
2	**2**	1	15
3	**3**	1	75
4	**4**	1	71
5	**3**	16	>99

[a] Conditions: 1 mol% cat.; 0.5 mmol of HBPin; 0.5 mmol of diphenylacetonitrile. [b] Conversions were determined by ^{1}H NMR spectroscopy by relative integration of the resonances of the HBPin and products and were based on HBPin.

CO$_2$

CO_2 + 3 HBPin $\xrightarrow[\text{60 °C, 16 h, THF-}d_8]{\text{1 mol% of }\mathbf{3}}$ H$_3$COBPin + PinB–O–BPin

57%

Isocyanates

RNCO + 3 HBPin $\xrightarrow[\text{60 °C, 16 h, C}_6\text{D}_6]{\text{1 mol% of }\mathbf{3}}$ R–N(CH$_3$)BPin + PinB–O–BPin

>99%   >99%   >99%   >99%

>99%   >99%   >99%[a]   >99%[b]

Esters

RC(O)OR' + 2 HBPin $\xrightarrow[\text{60 °C, 16 h, C}_6\text{D}_6]{\text{1 mol% of }\mathbf{3}}$ ROCH$_2$BPin + R'OBPin

56%   57%

89%   >99%   >99%   >99%

Nitriles

RCN + 2 HBPin $\xrightarrow[\text{60 °C, 1 h, C}_6\text{D}_6]{\text{1 mol% of }\mathbf{3}}$ R–CH$_2$–N(BPin)$_2$

75%   >99%   >99%   >99%

>99%   >99%   >99%   >99%   >99%   >99%

Scheme 2 Substrate scope of the hydroboration reactions catalyzed by complex **3**. The percentages correspond to the substrate conversion based on HBPin. For the indicated isocyanate substrates, a mixture of the methylene and methyl boramidate products was observed in a [a] 1 : 3.6 and [b] 1 : 2.1 ratio.

midate products along with the formation of PinBOBPin (Fig. S19–S26 in the ESI†). The formation of the products was confirmed by comparing the ^{1}H NMR resonances with those reported in the literature.[12,29] When using isocyanate substrates bearing mesityl and diisopropylphenyl substituents, the formation of methylene boramidate products was also observed in methylene : methyl ratios of 1 : 3.6 and 1 : 2.1, respectively. This observation is likely due to the very high stereochemical hindrance imparted by these substrates.

Regarding ester substrates (Fig. S27–S32 in the ESI†), 1 mol% of complex **3** catalyzed the hydroboration of ethyl and methyl benzoate, forming PhCH$_2$OBPin (along with H$_3$CH$_2$COBPin for ethyl benzoate and H$_3$COBPin for methyl benzoate) in conversions of 57% and 56%, respectively. The hydroborations of the ester substrates ethyl acetate and diethyl oxalate were smoothly catalyzed by complex **3**, achieving 89 and >99% conversions, respectively. Cyclic esters, γ-butyrolactone and ε-caprolactone, were also quantitatively hydroborated in the present study. The formation of products was confirmed by comparing the ^{1}H NMR resonances with those reported in the literature.[17a] The catalyst system comprising 1 mol% of complex **3** also promoted the hydroborative deoxygenation of *N,N*-diethylbenzamide to *N*-benzyl-*N*-ethylethanamine in a near-quantitative conversion at 60 °C in C$_6$D$_6$ after 16 h (Fig. S33 in the ESI†). The formation of this product, along with PinBOBPin, was confirmed by comparing its ^{1}H NMR spectrum with that reported in the literature.[50] This latter result is significant, since deoxygenation of tertiary amides *via* hydroboration is a rare occurrence in the literature.[50]

Complex **3** also catalyzed the dihydroboration of nitrile substrates (Fig. S34–S43 in the ESI†). With this system, a number of aliphatic and electronically differentiated aromatic substrates were successfully dihydroborated. Also, complex **3** catalyzed the chemoselective dihydroboration of 2-(bromomethyl) benzonitrile. The formation of the products was confirmed by comparing the ^{1}H NMR resonances with those reported in the literature.[25b]

No catalytic activity was ever observed when performing the reactions at 25 °C or in the absence of catalyst for all preliminarily tested substrates (Fig. S44 in the ESI†). Complexes **1–4** did not catalyze the hydroboration of the heterocyclic substrate pyridine.

In order to evaluate the relative reactivity of the different substrate families when exposed to the present hydroboration conditions, selected competitive experiments were performed (Scheme 3A). When performing the competitive hydroboration with 1-isocyanatonaphthalene or benzonitrile with ethyl benzoate, only the products resulting from the conversion of isocyanate or nitrile substrates were observed. On the other hand, when performing the competitive hydroboration between 1-isocyanatonaphthalene and benzonitrile, a mixture of products was observed, in which the dihydroboration product of benzonitrile corresponds to 36% of the mixture, while 64% resulted from the conversion of 1-isocyanatonaphthalene, forming the formyl and methyl boramidate (along with PinBOBPin) products in a 0.8 : 1 ratio. The spectra relevant to the competition experiments are presented in Fig. S45–S47 in the ESI.† These results show that the present catalyst system is chemoselective toward nitrile or isocyanate substrates in comparison with ester ones.

The catalytic hydroboration reactions of *tert*-butyl isocyanate, ethyl benzoate and diphenylacetonitrile using 5 mol% of complex **3** were also performed (Scheme 3B), with the corresponding magnified versions of the ^{11}B NMR spectra being pre-
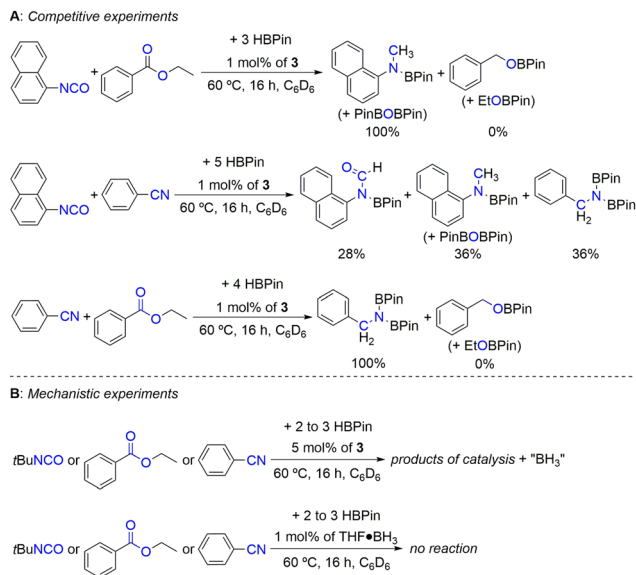
**Scheme 3** Competitive (A) and mechanistic (B) experiments. The percentages correspond to the products' ratio.

sented in Fig. S48 in the ESI.† The ^{11}B NMR spectra acquired from these reactions revealed the appearance of quartet resonances centered at −12 ppm ($^1J_{BH}$ = 99 Hz), indicative of the presence of BH$_3$.[51] The observation of BH$_3$ in the reaction mixtures arises from the dissociation of the borohydride co-ligands in complex **3**, readily forming the respective zinc dihydride intermediate [(**L3**)ZnH$_2$]. The formation and structure of this intermediate have already been discussed in a previous publication.[41] It may not be ruled out that the BH$_3$ formed during the catalytic reactions is trapped by the coordinative pressure of the substrates, leading to the formation of substrate·BH$_3$ Lewis pairs. In fact, for the *tert*-butyl isocyanate substrate, two further triplets ($^1J_{BH}$ = 119 Hz) appeared in the ^{11}B NMR spectrum, indicating that "BH$_2$" species are present, likely originating from stoichiometric hydroboration reactions with BH$_3$ formed during the catalytic initiation process.

The spontaneous liberation of BH$_3$ from complex **3** was never observed, not even after prolonged heating at 60 °C. To discard the possibility of substrate·BH$_3$ adducts operating as catalysts themselves, the catalytic hydroborations of CO$_2$, *tert*-butyl isocyanate, ethyl benzoate and diphenylacetonitrile with HBPin in the presence of 1 mol% of THF·BH$_3$ were performed (Scheme 3B). In our hands, no catalytic activity was ever observed. In fact, even though BH$_3$ adducts have been known to catalyze the hydroboration of nitriles with HBPin, they did so in very low yields.[52] Control reactions performed with 1 mol% of THF·BH$_3$ in the presence of **L3** also did not lead to any catalytic activity. In addition, reactions of complex **3** with 1 bar of CO$_2$ or 5 equivalents of 1,3-difluoro-5-isocyanatobenzene or 4-fluorobenzonitrile were performed, with the respective ^{1}H NMR spectra being presented in Fig. S49 in the ESI.† Even though such reactions led to complex mixtures of products, the formation of new complexes was evident and the appear-

ance of deshielded singlet resonances at 7.81–9.16 ppm was observed, attributed to zinc formate (for CO$_2$), formamide (for 1,3-difluoro-5-isocyanatobenzene) or azavinylidene (for 4-fluorobenzonitrile) proton resonances. This indicates the occurrence of substrate insertion reactions in the putative zinc dihydride intermediate [(**L3**)ZnH$_2$], likely formed upon liberation of BH$_3$ from complex **3**. Such deshielded singlet resonances have been detected in zinc formate (8.33 ppm),[41] formamide (7.93 ppm)[29] and azavinylidene (9.59 ppm)[30e] complexes.

In order to gain further insight into the activation of the catalysts, the spontaneous liberation of BH$_3$ from complex **3** and the reactions of complex **3** with the different families of substrates, giving rise to the putative dihydride complex [(**L3**)ZnH$_2$] and corresponding substrate·BH$_3$ adducts, were studied by DFT calculations[53] and the respective Gibbs energy balances were established (Scheme 4).

By looking at the energy balances determined by DFT calculations, the spontaneous liberation of BH$_3$ from complex **3** yielding complex [(**L3**)ZnH$_2$]$_{free}$ is less unfavorable than that induced by the different substrate molecules with a free energy balance of ΔG = 28 kcal mol^{-1}. This value is further reduced to 20 kcal mol^{-1} when considering that the spontaneous liberation of BH$_3$ from complex **3** yields complex [(**L3**)ZnH$_2$]$_{capped}$, in which the pending borane intramolecularly stabilizes one of the hydride ligands. The structure of complex [(**L3**)ZnH$_2$]$_{capped}$ has been discussed in a previous publication.[41] For all other substrate families, except nitriles, the liberation and subsequent trapping processes of BH$_3$ using CO$_2$, *tert*-butyl isocyanate and ethyl benzoate are highly unfavored, resulting in Gibbs energies in the range of 45–62 kcal mol^{-1}. The presented energy balances are, thus, in line with the systematic
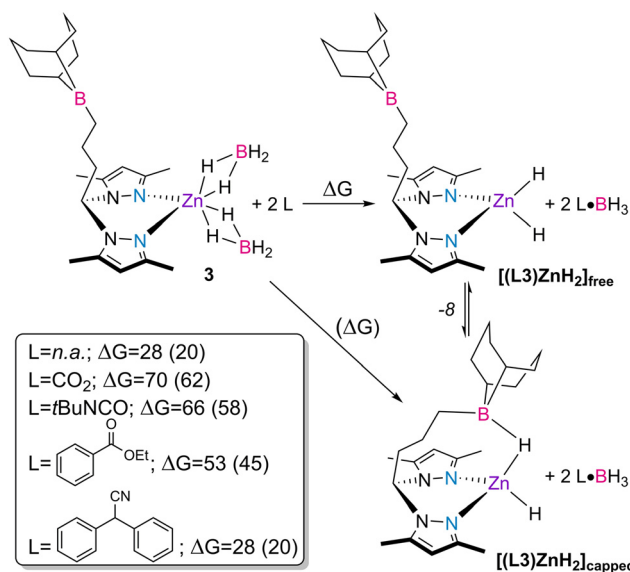
Scheme 4 Gibbs energy balances (in kcal mol^{-1}) for the reactions involving the liberation of BH$_3$ from the bis(κ^2-borohydride) complex **3**, yielding complex [(**L3**)ZnH$_2$]$_{free}$ or [(**L3**)ZnH$_2$]$_{capped}$ (numbers in parentheses) determined by DFT calculations.

observation of BH_3 over the course of the catalytic reactions, regardless of the type of substrate used. In addition, they further corroborate the increased catalytic activity observed in the borane-substituted catalysts **3** and **4** in comparison with the unfunctionalized complexes **1** and **2**, giving the favorable formation of the capped form of the complex.

Given the experimental and theoretical information described above, as well as the conclusions taken from our previous work,[41] a mechanistic discussion may be proposed (Scheme 5).

The activation step in the mechanistic hypothesis is common to all substrate families: elimination of BH_3 from the κ^2-borohydride ligands in the complexes, giving rise to the formation of **[LZnH₂]** intermediates. The **[LZnH₂]** intermediates bearing the borane-functionalized ligands **L3** and **L4** may either exhibit the borane in a tri-coordinated, free conformation or where the borane is inter- (via dimerization) or intramolecularly stabilizing one of the hydride ligands.[41] Subsequently, the substrates undergo insertion into the

[LZnH₂] intermediates, forming the respective formate (**[LZn(OCHO)₂]**, for CO_2), formamide (**[LZn(N(R)CHO)₂]**, for isocyanates), methanolate (**[LZn(OCH₂(R)OR')₂]**, for esters) and azavinylidene (**[LZn(N=CH(R))₂]**, for nitriles) intermediates.

In the case of the hydroboration of CO_2 and isocyanates (Scheme 5A), the formate or formamide intermediates, respectively, resulting from their insertion into the **[LZnH₂]** intermediates, give rise, upon reaction with an excess amount HBPin, to the generation of the formyl or formamide compounds HCOEBPin (E being O or N(R)), regenerating **[LZnH₂]** (Scheme 5A, cycle **I**). Compounds HCOEBPin undergo further insertion reactions into the Zn–H bonds of the **[LZnH₂]** intermediates, generating complexes of type **[LZn(OCH₂EBPin)₂]** (Scheme 5A, cycle **II**). Intermediate complexes **[LZn(OCH₂EBPin)₂]** may further react with HBPin, leading to the formation of $H_3CEBPin$ along with intermediates **[LZn(OBPin)₂]**. Complexes **[LZn(OBPin)₂]** give rise to PinBOBPin by further reaction with HBPin, again regenerating **[LZnH₂]** (Scheme 5A, cycle **III**). This mechanism was originally proposed by Trovitch[7] and was analogously reported by us in our previous study concerned with the hydroboration of CO_2 catalyzed by complexes **[(L1–4)ZnCl₂]**/KHBEt₃,[41] and is supported by the fact that the present catalyst systems give rise to methyl-level products.

With respect to the hydroboration of esters (Scheme 5B), further reaction of the methanolate intermediates **[LZn(OCH₂(R)OR')₂]** with HBPin would lead to the formation of compounds PinBOCH₂(R)OR' and regeneration of intermediates **[LZnH₂]** (Scheme 5B, cycle **I**). Subsequent reaction of PinBOCH₂(R)OR' and **[LZnH₂]** would likely induce an ether cleavage reaction, generating intermediate **[LZn(OCH₂R)₂]** and compounds R'OBPin, the latter products being systematically observed in all catalytic reactions. The reaction of intermediate complex **[LZn(OCH₂R)₂]** with HBPin would also give rise to compounds PinBOCH₂R and regenerate the dihydride intermediates **[LZnH₂]** (Scheme 5B, cycle **II**). This ester hydroboration mechanism has been reported by Nembenna and coworkers.[17]

Lastly, the hydroboration of nitriles (Scheme 5C) and the reaction of the azavinylidene intermediates **[LZn(N=CH(R))₂]** with HBPin would give rise to the imine PinBN=CH(R) and regeneration of the **[LZnH₂]** intermediates (Scheme 5C, cycle **I**). The imine PinBN=CH(R) likely undergoes a facile insertion reaction into the Zn–H bonds of the **[LZnH₂]** intermediates, generating the intermediate amido complexes **[LZn(NCH₂R)₂]**. Such amido complexes may react with HBPin and give rise to products PinBNCH₂R and the regeneration of the **[LZnH₂]** active species (Scheme 5C, cycle **II**).

The role of the appended boranes in complexes **3** and **4** is that of kinetically stabilizing intermediates in all catalytic cycles by means of establishing Lewis pairs between hydrogen/oxygen/nitrogen-based ligands and the respective borane functions via Zn–H–B/Zn–O–B/Zn–N–B interactions. These interactions may facilitate insertion and σ-bond metathesis reactions by weakening the respective Zn–H/Zn–O/Zn–N bonds.
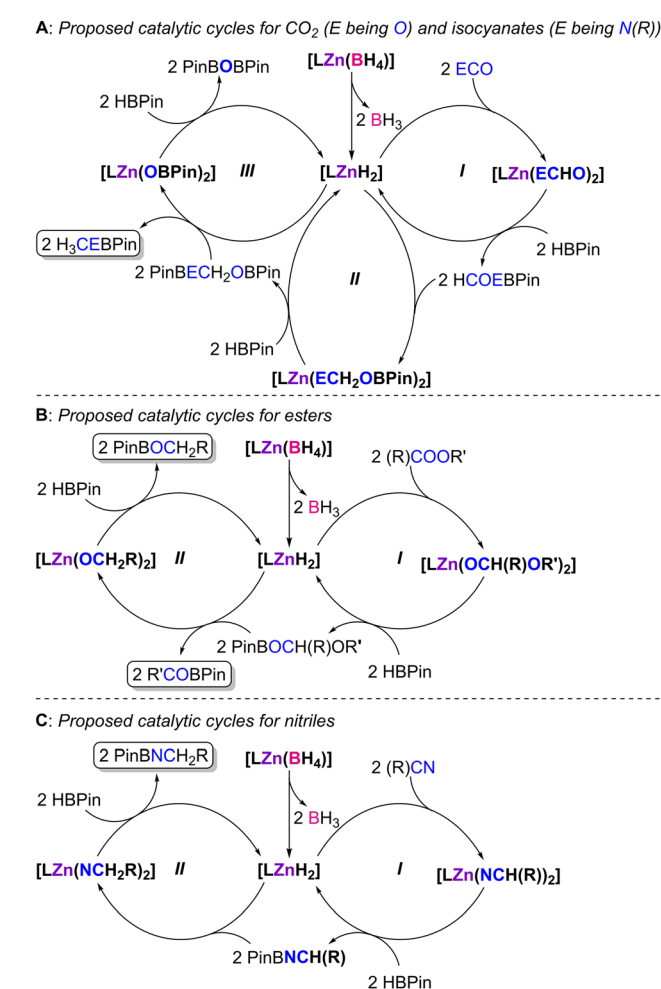
Scheme 5 Mechanistic proposal for the hydroboration of CO_2 and isocyanates (A), esters (B) and nitriles (C) with HBPin catalyzed by complexes **1–4**, where L denotes ligands **L1–4**.

Conclusions

In this work, new bis(κ^2-borohydride) zinc complexes of borane-functionalized heteroscorpionate ligands served as catalysts for the hydroboration of a broad scope of substrates.

Four new bis(κ^2-borohydride) zinc complexes **1–4** were synthesized. Complexes **1** and **2** contained unfunctionalized and allyl-functionalized bis(3,5-dimethylpyrazolyl)methane ligands, while complexes **3** and **4** contained borane functionalities on these scaffolds. Complexes **1–4** were characterized by NMR spectroscopy, FTIR spectroscopy and elemental analysis while complex **3** was additionally characterized by single-crystal X-ray diffraction. All complexes displayed the κ^2-coordination mode of borohydride, as confirmed by the spectroscopic techniques used.

The new complexes were used as catalysts in the hydroboration of a series of unsaturated substrates containing heteroatoms, namely CO_2 at 1 bar, *tert*-butyl isocyanate, and ethyl benzoate and the dihydroboration of diphenylacetonitrile at 60 °C with 1 mol% of catalyst loading. The borane-functionalized complexes **3** and **4** achieved conversions of 29–99% and, as a common feature, exhibited an average 5-fold increase in their catalytic activities in comparison with the unfunctionalized complexes **1** and **2**. In the case of CO_2 and isocyanates, the methylated products (along with PinBOBPin) were preferred after 16 h. In addition, 1 mol% of complex **3** catalyzed the hydroboration of several isocyanates, esters and nitriles with yields in the range of 56–99%.

The catalytic competence of the new complexes is dependent on the release of BH_3 from the borohydride ligands, as confirmed by a set of experimental and theoretical observations. This generates dihydride zinc complexes, through which catalytic turnover takes place. The borane functionalities in complexes **3** and **4** provide a catalytic advantage because they are able to establish Lewis pairs with oxygen- and nitrogen-containing catalytic intermediates.

Data availability

The data supporting this article have been included as part of the ESI.†

Conflicts of interest

The authors declare no conflict of interest.

Acknowledgements

References

1 (a) V. P. Ananikov and M. Tanaka, *Hydrofunctionalization*, Springer, 2013, vol. 43; (b) A. J. J. Lennox and G. C. Lloyd-Jones, *Chem. Soc. Rev.*, 2014, **43**, 412–443.

2 (a) C. Erken, A. Kaithal, S. Sen, T. Weyhermüller, M. Hölscher, C. Werlé and W. Leitner, *Nat. Commun.*, 2018, **9**, 4521–4529; (b) S. Kostera, M. Peruzzini, K. Kirchner and L. Gonsalvi, *ChemCatChem*, 2020, **12**, 4625–4631; (c) P. Ghosh and A. J. von Wangelin, *Angew. Chem., Int. Ed.*, 2021, **60**, 16035–16043.

3 (a) G. Jin, C. G. Werncke, Y. Escudié, S. Sabo-Etienne and S. Bontemps, *J. Am. Chem. Soc.*, 2015, **137**, 9563–9566; (b) S. Lau, C. B. Provis-Evans, A. P. James and R. L. Webster, *Dalton Trans.*, 2021, **50**, 10696–10700; (c) H. Gao, J. Jia, C.-H. Tung and I. Wang, *Organometallics*, 2023, **42**, 944–951.

4 S. R. Tamang and M. Findlater, *Dalton Trans.*, 2018, **47**, 8199–8203.

5 H.-W. Suh, L. M. Guard and N. Hazari, *Polyhedron*, 2014, **84**, 37–43.

6 R. Shintani and K. Nozaki, *Organometallics*, 2013, **32**, 2459–2462.

7 R. Pal, T. L. Groy and R. J. Trovitch, *Inorg. Chem.*, 2015, **54**, 7506–7515.

8 (a) S. Bontemps, L. Vendier and S. Sabo-Etienne, *Angew. Chem., Int. Ed.*, 2012, **51**, 1671–1674; (b) M. J. Sgro and D. W. Stephan, *Angew. Chem., Int. Ed.*, 2012, **51**, 11343–11345; (c) S. Bontemps and S. Sabo-Etienne, *Angew. Chem., Int. Ed.*, 2013, **52**, 10253–10255; (d) S. Bontemps, L. Vendier and S. Sabo-Etienne, *J. Am. Chem. Soc.*, 2014, **136**, 4419–4425; (e) C. K. Ng, J. Wu, T. S. A. Hor and H.-K. Luo, *Chem. Commun.*, 2016, **52**, 11842–11845; (f) L. Li, H. Zhu, L. Liu, D. Song and M. Lei, *Inorg. Chem.*, 2018, **57**, 3054–3060.

9 H.-W. Suh, L. M. Guard and N. A. Hazari, *Chem. Sci.*, 2014, **5**, 3859–3872.

10 (a) M. D. Anker, M. Arrowsmith, P. Bellham, M. S. Hill, G. Kociok-Köhn, D. J. Liptrot, M. F. Mahon and C. Weetman, *Chem. Sci.*, 2014, **5**, 2826–2830; (b) J. A. B. Abdalla, I. M. Riddlestone, R. Tirfoin and S. Aldridge, *Angew. Chem., Int. Ed.*, 2015, **54**, 5098–5102; (c) Z. Lu, H. Hausmann, S. Becker and H. A. Wegner, *J. Am. Chem. Soc.*, 2015, **137**, 5332–5335; (d) T. J. Hadlington, C. E. Kefalidis, L. Maron and C. Jones, *ACS Catal.*, 2017, **7**, 1853–1859; (e) X. Cao, W. Wang, K. Lu, W. Yao, F. Xue and M. Ma, *Dalton Trans.*, 2020, **49**, 2776–2780; (f) C.-C. Chia, W.-C. Teo, N. Cham, S. Y.-F. Ho, Z.-H. Ng, H.-M. Toh, N. Mézailles and C.-W. So, *Inorg. Chem.*, 2021, **60**, 4569–4577; (g) J. Fan, J.-Q. Mah, M.-C. Yang, M.-D. Su and C.-W. So, *J. Am. Chem. Soc.*, 2021, **143**, 4993–5002; (h) B. Yan, S. Dutta, X. Ma, C. Ni, D. Koley, Z. Yang and H. W. Roesky, *Dalton Trans.*, 2022, **51**, 6756–6765.

11 M. R. Espinosa, D. J. Charboneau, A. G. de Oliveira and N. Hazari, *ACS Catal.*, 2019, **9**, 301–314.

12 K. A. Gudun, S. Tussupbayev, A. Slamovac and A. Y. Khalimon, *Org. Biomol. Chem.*, 2022, **20**, 6821–6830.

13 L. E. English, T. M. H. Downie, C. L. Lyall, M. F. Mahon, C. L. McMullin, S. E. Neale, C. M. Saunders and D. J. Liptrot, *Chem. Commun.*, 2023, **59**, 1074–1077.

14 V. K. Pandey, S. Sahoo and A. Rit, *Chem. Commun.*, 2022, **58**, 5514–5517.

15 (*a*) Y. Yang, M. D. Anker, J. Fang, M. F. Mahon, L. Maron, C. Weetman and M. S. Hill, *Chem. Sci.*, 2017, **8**, 3529–3537; (*b*) N. Sarkar, R. K. Sahoo and S. Nembenna, *Eur. J. Org. Chem.*, 2022, e202200941; (*c*) C. Ni, X. Ma, Z. Yang and H. W. Roesky, *ChemistrySelect*, 2022, **7**, e202202878; (*d*) J. Shi, M. Luo, X. Zhang, T. Yuan, X. Chen and M. Ma, *Org. Biomol. Chem.*, 2023, **21**, 3628–3635.

16 K. Makarov, I. Ritacco, N. Fridman, L. Caporaso and M. S. Eisen, *ACS Catal.*, 2023, **13**, 11798–11814.

17 (*a*) N. Sarkar, R. K. Sahoo and S. Nembenna, *Chem. – Eur. J.*, 2023, **29**, e202203023; (*b*) Y. Zheng, X. Zhu, X. Xu, S. Zhou, W. Lua and M. Xue, *New J. Chem.*, 2023, **47**, 19367–19371.

18 (*a*) T. T. Nguyen, J.-H. Kim, S. Kim, C. Oh, M. Flores, T. L. Groy, M.-H. Baik and R. J. Trovitch, *Chem. Commun.*, 2020, **56**, 3959–3962; (*b*) M. R. Elsby, C. Oh, M. Son, S. Y. H. Kim, M.-H. Baik and R. T. Baker, *Chem. Sci.*, 2022, **13**, 12550–12559.

19 (*a*) A. R. Bazkiaei, M. Wiseman and M. Findlater, *RSC Adv.*, 2021, **11**, 15284–15289; (*b*) T. Komuro, K. Hayasaka, K. Takahashi, N. Ishiwata, K. Yamauchi, H. Tobita and H. Hashimoto, *Dalton Trans.*, 2024, **53**, 4041–4047.

20 (*a*) A. D. Ibrahim, S. W. Entsminger and A. R. Fout, *ACS Catal.*, 2017, **7**, 3730–3734; (*b*) H. Ben-Daat, C. L. Rock, M. Flores, T. L. Groy, A. C. Bowman and R. J. Trovitch, *Chem. Commun.*, 2017, **53**, 7333–7336; (*c*) C. Ghosh, S. Kim, M. R. Mena, J.-H. Kim, R. Pal, C. L. Rock, T. L. Groy, M.-H. Baik and R. J. Trovitch, *J. Am. Chem. Soc.*, 2019, **141**, 15327–15337; (*d*) J. Pecak, W. Eder, B. Stöger, S. Realista, P. N. Martinho, M. J. Calhorda, W. Linert and K. Kirchner, *Organometallics*, 2020, **39**, 2594–2601; (*e*) K. A. Gudun, A. Slamova, D. Hayrapetyan and A. Y. Khalimon, *Chem. – Eur. J.*, 2020, **26**, 4963–4968; (*f*) C. Li, S. Song, Y. Li, C. Xu, Q. Luo, Y. Guo and X. Wang, *Nat. Commun.*, 2021, **12**, 3813–3820.

21 (*a*) S. Ataie and R. T. Baker, *Inorg. Chem.*, 2022, **61**, 19998–20007; (*b*) M. Afandiyeva, X. Wu, W. W. Brennessel, A. A. Kadam and C. R. Kennedy, *Chem. Commun.*, 2023, **59**, 13450–13453.

22 (*a*) J. B. Geri and N. K. Szymczak, *J. Am. Chem. Soc.*, 2015, **137**, 12808–12814; (*b*) A. Kaithal, B. Chatterjee and C. Gunanathan, *J. Org. Chem.*, 2016, **81**, 11153–11161; (*c*) T. Kitano, T. Komuro and H. Tobita, *Organometallics*, 2019, **38**, 1417–1420.

23 V. K. Pandey, C. S. Tiwari and A. Rit, *Org. Lett.*, 2021, **23**, 1681–1686.

24 (*a*) C. Weetman, M. D. Anker, M. Arrowsmith, M. S. Hill, G. Kociok-Köhn, D. J. Liptrot and M. F. Mahon, *Chem. Sci.*, 2016, **7**, 628–641; (*b*) A. Harinath, J. Bhattacharjee and T. K. Panda, *Adv. Synth. Catal.*, 2019, **361**, 850–857; (*c*) W. Liu, Y. Ding, D. Jin, Q. Shen, B. Yan, X. Ma and Z. Yang, *Green Chem.*, 2019, **21**, 3812–3815; (*d*) Y. Ding, X. Ma, Y. Liu, W. Liu, Z. Yang and H. W. Roesky, *Organometallics*, 2019, **38**, 3092–3097; (*e*) N. Sarkar, S. Bera and S. Nembenna, *J. Org. Chem.*, 2020, **85**, 4999–5009; (*f*) P. Ghosh and A. J. von Wangelin, *Org. Chem. Front.*, 2020, **7**, 960–966; (*g*) D. Bedi, A. Brar and M. Findlater, *Green Chem.*, 2020, **22**, 1125–1128; (*h*) B. Yan, X. He, C. Ni, Z. Yang and X. Ma, *ChemCatChem*, 2021, **13**, 851–854; (*i*) J. Peng, Y. Song, Y. Wang, Z. Liu and X. Chen, *Org. Chem. Front.*, 2022, **9**, 1536–1540; (*j*) J. E. Seok, H. T. Kim, J. Kim, J. H. Lee, A. K. Jaladi, H. Hwang and D. K. An, *Asian J. Org. Chem.*, 2022, **11**, e202200405.

25 (*a*) Z. Huang, S. Wang, X. Zhu, Q. Yuan, Y. Wei, S. Zhou and X. Mu, *Inorg. Chem.*, 2018, **57**, 15069–15078; (*b*) S. Saha and M. S. Eisen, *ACS Catal.*, 2019, **9**, 5947–5956.

26 Z. Du, B. Behera, A. Kumar and Y. Ding, *J. Organomet. Chem.*, 2021, **950**, 121982.

27 (*a*) J. Bhattacharjee, D. Bockfeld and M. Tamm, *J. Org. Chem.*, 2022, **87**, 1098–1109; (*b*) R. Narvariya, S. Das, S. Mandal, A. Jain and T. K. Panda, *Eur. J. Inorg. Chem.*, 2023, **26**, e202300247; (*c*) R. Kumar, K. Bano, M. Choudhary, J. Sharma, K. Pal, S. K. Singh and T. K. Panda, *Organometallics*, 2023, **42**, 2216–2227; (*d*) H. J. Han, S. Y. Park, S. E. Jeon, J. S. Kwak, J. H. Lee, A. K. Jaladi, H. Hwang and D. K. An, *Molecules*, 2023, **28**, 7090–7111.

28 (*a*) D. Mukherjee, A.-K. Wiegand, T. P. Spaniol and J. Okuda, *Dalton Trans.*, 2017, **46**, 6183–6186; (*b*) X. Wang, K. Chang and X. Xu, *Dalton Trans.*, 2020, **49**, 7324–7327; (*c*) R. Chambenahalli, R. M. Bhargav, K. N. McCabe, A. P. Andrews, F. Ritter, J. Okuda, L. Maron and A. Venugopal, *Chem. – Eur. J.*, 2021, **27**, 7391–7401; (*d*) D. G. Shlian, E. Amemiya and G. Parkin, *Chem. Commun.*, 2022, **58**, 4188–4191.

29 R. K. Sahoo, N. Sarkar and S. Nembenna, *Angew. Chem., Int. Ed.*, 2021, **60**, 11991–12000.

30 (*a*) S. Das, J. Bhattacharjee and T. K. Panda, *New J. Chem.*, 2019, **43**, 16812–16818; (*b*) X. Wang and X. Xu, *RSC Adv.*, 2021, **11**, 1128–1133; (*c*) S. Ataie, J. S. Ovens and R. T. Baker, *Chem. Commun.*, 2022, **58**, 8266–8269; (*d*) S. Mondal, T. Singh, S. Baguli, S. Ghosh and D. Mukherjee, *Chem. – Eur. J.*, 2023, **29**, e202300508; (*e*) R. K. Sahoo, S. Rajput, S. Dutta, K. Sahu and S. Nembenna, *Organometallics*, 2023, **42**, 2293–2303; (*f*) S. Ataie and R. T. Baker, *ChemCatChem*, 2023, **15**, e202300649.

31 H. Karmakar, G. S. Kumar, K. Pal, V. Chandrasekhar and T. K. Panda, *Dalton Trans.*, 2024, **53**, 10592–10602.

32 M. H. Drover, *Chem. Soc. Rev.*, 2022, **51**, 1861–1880.

33 D. Specklin, M.-C. Boegli, A. Coffinet, L. Escomel, L. Vendier, M. Grellier and A. Simonneau, *Chem. Sci.*, 2023, **14**, 14262–14270.

34 (*a*) A. J. M. Miller, J. A. Labinger and J. E. Bercaw, *J. Am. Chem. Soc.*, 2008, **130**, 11874–11875; (*b*) T. G. Ostapowicz, C. Merkens, M. Hölscher, J. Klankermayer and W. Leitner, *J. Am. Chem. Soc.*, 2013, **135**, 2104–2107.

35 (a) M. L. Clapson and M. W. Drover, *Nat. Synth.*, 2022, **1**, 267–268; (b) M. L. Clapson, H. Sharma, J. A. Zurakowski and M. W. Drover, *Chem. – Eur. J.*, 2023, **29**, e202203763; (c) J. A. Zurakowski, K. R. Brown and M. W. Drover, *Inorg. Chem.*, 2023, **62**, 7053–7060.

36 B. J. H. Austen, M. L. Clapson and M. W. Drover, *RSC Adv.*, 2023, **13**, 19158–19163.

37 (a) J. J. Kiernicki, M. Zeller and N. K. Szymczak, *J. Am. Chem. Soc.*, 2017, **139**, 18194–18197; (b) J. J. Kiernicki, J. P. Shanahan, M. Zeller and N. K. Szymczak, *Chem. Sci.*, 2019, **10**, 5539–5545; (c) J. J. Kiernicki, E. E. Norwine, M. Zeller and N. K. Szymczak, *Chem. Commun.*, 2019, **55**, 11896–11899; (d) J. J. Kiernicki, M. Zeller and N. K. Szymczak, *Organometallics*, 2021, **40**, 2658–2665.

38 (a) E. E. Norwine, J. J. Kiernicki, M. Zeller and N. K. Szymczak, *J. Am. Chem. Soc.*, 2022, **144**, 15038–15046; (b) E. E. Norwine, J. J. Kiernicki, M. Zeller and N. K. Szymczak, *Inorg. Chem.*, 2024, **63**, 18519–18523.

39 H. Song and N. K. Szymczak, *Angew. Chem., Int. Ed.*, 2024, e202411099.

40 (a) V. Chugh, B. Chatterjee, W.-C. Chang, H. H. Cramer, C. Hindemith, H. Randel, T. Weyhermüller, C. Farès and C. Werlé, *Angew. Chem., Int. Ed.*, 2022, **61**, e202205515; (b) S. Jena, L. Frenzen, V. Chugh, J. Wu, T. Weyhermüller, A. A. Auer and C. A. Werlé, *J. Am. Chem. Soc.*, 2023, **145**, 27922–27932.

41 T. F. C. Cruz, V. Loupy and L. F. Veiros, *Inorg. Chem.*, 2024, **63**, 8244–8256.

42 J. Reedijk and J. Verbiest, *Transition Met. Chem.*, 1979, **4**, 239–243.

43 S. Hermanek, *Chem. Rev.*, 1992, **92**, 325–362.

44 G. W. Kramer and H. C. Brown, *J. Organomet. Chem.*, 1974, **73**, 1–15.

45 T. J. Marks and J. R. Kolb, *Chem. Rev.*, 1977, **77**, 263–293.

46 L. Yang, D. R. Powell and R. P. Houser, *Dalton Trans.*, 2007, 955–964.

47 (a) D. Cremer and J. A. Pople, *J. Am. Chem. Soc.*, 1975, **97**, 1354–1358; (b) R. Puerta-Oteo, M. V. Jiménez, F. J. Lahoz, F. J. Modrego, V. Passarelli and J. J. Pérez-Torrente, *Inorg. Chem.*, 2018, **57**, 5526–5543.

48 (a) Q. Gu, L. Gao, Y. Guo, Y. Tan, Z. Tang, K. S. Wallwork, F. Zhangc and X. Yu, *Energy Environ. Sci.*, 2012, **5**, 7590–7600; (b) S. M. I. Al-Rafia, P. A. Lummis, A. K. Swarnakar, K. C. Deutsch, M. J. Ferguson, R. McDonald and E. Rivard, *Aust. J. Chem.*, 2013, **66**, 1235–1245; (c) K. Kadota, N. T. Duong, Y. Nishiyama, E. Sivaniah, S. Kitagawad and S. Horike, *Chem. Sci.*, 2019, **10**, 6193–6198.

49 S. R. Tamang and M. Findlater, *Dalton Trans.*, 2018, **47**, 8199–8203.

50 (a) P. Ye, Y. Shao, X. Ye, F. Zhang, R. Li, J. Sun, B. Xu and J. Chen, *Org. Lett.*, 2020, **22**, 1306–1310; (b) G. S. Kumar, J. Bhattacharjee, K. Kumari, S. Moorthy, A. Bandyopadhyay, S. K. Singh and T. K. Panda, *Polyhedron*, 2022, **219**, 115784; (c) A. Adilkhanova, V. F. Frolova, A. Yessengazin, Ö. Öztopçu, K. A. Gudun, M. Segizbayev, N. A. Matsokin, A. Dmitrienko, M. Pilkington and A. Y. Khalimon, *Dalton Trans.*, 2023, **52**, 2872–2886.

51 (a) A. D. Bage, T. A. Hunt and S. P. Thomas, *Org. Lett.*, 2020, **22**, 4107–4112; (b) B. Yan, X. Ma, Z. Pang and Z. Yang, *New J. Chem.*, 2023, **47**, 3202–3206.

52 (a) F. Meger, A. C. W. Kwok, F. Gilch, D. R. Willcox, A. J. Hendy, K. Nicholson, A. D. Bage, T. Langer, T. A. Hunt and S. P. Thomas, *Beilstein J. Org. Chem.*, 2022, **18**, 1332–1337; (b) R. Kumar, R. K. Meher, J. Sharma, A. Sal and T. K. Panda, *Org. Lett.*, 2023, **25**, 7923–7927.

53 (a) G. R. Parr and W. Yang, *Density Functional Theory of Atoms and Molecules*, Oxford University Press, New York, 1989; (b) Calculations performed at the PBE0-D3/6-311++G*(d,p)// PBE0/(SDD*,6-31G(d,p)) level using the GAUSSIAN 09 package. Solvent effects (benzene) were considered using the PCM/SMD model. A full account of the computational details and a complete list of references are provided in the ESI.†